

Abundances of the rare-earth elements in Procyon

K. Kato¹ and K. Sadakane²

¹ Osaka Electric-Science Museum, Shinmachi, Nishi-ku, Osaka, 550 Japan

² Astronomical Institute, Osaka Kyoiku University, Minamikawahori-cho, Tennoji-ku, Osaka, 543 Japan

Received June 7, 1985; accepted June 2, 1986

Summary. A detailed abundance analysis of 13 rare-earth elements (La, Ce, Pr, Nd, Sm, Eu, Gd, Tb, Dy, Er, Tm, Yb, and Lu) has been carried out relative to the Sun for the bright F star Procyon (F5 IV–V). Weak and broadened rare-earth lines were analyzed by the method of spectrum synthesis. It was found that Procyon closely resembles the Sun in its rare-earth composition.

Key words: stars: abundances – stars: atmospheres – stars: individual

1. Introduction

The knowledge of stellar abundances of rare-earth elements (abbreviate to REE here) can provide information about the history of heavy element production in the Galaxy. However, detailed observational studies with high accuracy have not been done except for the Sun because of the following difficulties. First, spectral lines of REE are quite weak in normal stars and therefore they are easily affected by neighboring lines. In particular, most of the detectable lines lying at wavelengths below 4500 Å usually suffer from severe blending. Secondly, they are broadened by the hyperfine structure (abbreviate as hfs), by micro- and macro-turbulence, and by rotation. These effects make it difficult to get reliable equivalent widths of the lines. Thus high resolution, high signal-to-noise ratio spectra are indispensable for a detailed quantitative analysis. The bright and slowly rotating star Procyon is a suitable object for the study of weak rare-earth lines.

An abundance analysis of Procyon (α CMi, F5 IV–V) with a line-blanketed convective model atmosphere was carried out by the authors (Kato and Sadakane, 1982). They showed that the chemical abundances of nearly all the elements (Na to Pd) analyzed in Procyon are solar, while 5 rare-earths (Ce, Nd, Sm, Eu, and Dy) may be slightly underabundant with respect to the Sun. The latter result, however, was rather uncertain, because the measured equivalent widths were subject to fairly large observational errors due to their intrinsic weakness and also blending. Recently, Steffen (1985) has reported a fine analysis of 5 REE in Procyon, where an overabundance of La and slight underabundances of Ce, Nd, and Sm are found. His results are essentially the same as in our previous analysis. Besides these two fine analyses, the composition of 13 REE has been studied by

Send offprint requests to: K. Kato

Leushin and Sokolov (1982) based on the calculation of line profiles. They adopted an Edmonds' (1964) model of $T_{\text{eff}} = 6385$ K, $\log g = 4.107$, and found overabundances from 0.0 dex to 1.2 dex depending on the element.

In this paper REE lines in Procyon are analyzed in more detail by the method of spectrum synthesis.

2. Analysis

2.1. Line data

A total of 66 REE lines used here are given in Table 1, most of which were chosen from the list of Grevesse and Blanquet (1969) and some new lines were added. Solar REE line profiles measured on the *Jungfrau* Solar Atlas (Delbouille et al., 1973) were calculated together with the lines of Procyon to make the analysis self-consistent. For Procyon the line profiles of REE were measured from the *Spectrum Atlas of Procyon* (Griffin, 1979). The possible difference between the line profile “measured” on the *Procyon Atlas* and the “true” contour was investigated by Steffen (1985). He found that it is necessary for weak lines to apply a correction of about 10% to the “measured” equivalent width to obtain the “true” equivalent width. Effects of this correction on the final abundance will be discussed in the last section.

2.2. Atmospheric parameters

We use the same atmospheric parameters of Procyon as in our previous analysis: $T_{\text{eff}} = 6650$ K, $\log g = 4.0$, and a microturbulent velocity $\xi_t = 1.8$ km s⁻¹. As a broadening mechanism of a spectral line, we assume the Gaussian type “macro-turbulent” velocity field of $\exp(-v/\xi_{\text{mac}})^2$ (Gray, 1977). Reasonable agreements can be obtained when choosing $\xi_{\text{mac}} = 2.1$ km s⁻¹ and 5.0 km s⁻¹ for the Sun and Procyon, respectively. Effects of rotation and instrumental broadening are not fully taken into account here. Because of the practical difficulty in separating rotation, large-scale hydrodynamical motion, and instrumental profile in the spectrum of Procyon, we assume that these effects can be treated as the so called “macro-turbulence”. The “macro-turbulent” velocities obtained above for both stars include these factors.

Model atmospheres were taken from Holweger and Müller (1974) and Kurucz (1979) for the Sun and Procyon, respectively. Kurucz's line-blanketed solar model was also used for comparison.

Table 1. Line data used in the analysis and results. Column 1: Identification; Column 2: Wavelength (Å); Column 3: Lower excitation potential (eV); Column 4: $\log gf\epsilon$ value for Procyon on the scale of $\log \epsilon(H) = 12.0$; Column 5: $\log gf\epsilon$ value for the Sun; Column 6: Abundance relative to the Sun; Column 7: Weight (1 to 5); Column 8: Hyperfine structure (hfs); Column 9: Equivalent width (E.W.) in mÅ estimated from the $\log gf\epsilon$ in column 4; Column 10: Measured E.W. of Procyon taken from Kato and Sadakane (1982); Column 11: Solar E.W. estimated from the $\log gf\epsilon$ in column 5; Column 12: Measured solar E.W. taken from Grevesse and Blanquet (1966) and Moore et al. (1966)

Elmnt	λ (Å)	χ (eV)	$\log gf\epsilon$		[ϵ]	Wght	hfs	Computed & Measued EW			
			Procyon	Sun				Procyon		Sun	
La II 57	3988.52	0.40	+1.31	+1.34	-0.03	5	hfs	45		49	<44>
	3995.75	0.17	+1.05	+1.07	-0.02	5	hfs	36	37	39	<38>
	4042.91	0.92	+1.41	+1.50	-0.09	5		19	21	20	<18>
	4086.72	0.00	+1.06	+1.20	-0.14	4		40		38	42
	4322.51	0.17	+0.46	+0.49	-0.03	3	hfs	12		15	19
	4333.74	0.17	+1.03	+1.05	-0.02	2	hfs	37		39	42
	4522.37	1.24	+1.26	+1.26	0.00	1		9		8	<9>
	4662.51	0.00	-0.05	-0.03	-0.02	4		6	7	7	<5>
	4748.73	0.92	+0.64	+0.63	+0.01	2		5		4	4
	5122.99	0.32	+0.33	+0.35	-0.02	2		8	9	8	9
Ce II 58	4042.58	0.49	+1.51	+1.55	-0.04	5		10	9	11	10
	4068.84	0.70	+1.32	+1.34	-0.02	3		4		5	5
	4073.48	0.47	+1.78	+1.80	-0.02	5		17		17	15
	4083.23	0.69	+2.02	+2.06	-0.04	2		19		19	26
	4364.66	0.49	+1.46	+1.45	+0.01	3		9		9	14
	4382.17	0.68	+1.68	+1.70	-0.02	2		10	8	11	8
	4486.91	0.29	+1.35	+1.38	-0.03	2		11	10	12	15
	4523.08	0.51	+1.54	+1.57	-0.03	2		12	10	12	12
	4562.36	0.47	+1.72	+1.81	-0.09	2		17	18	19	20
	4628.16	0.51	+1.61	+1.68	-0.07	3		13	14	14	<14>
4773.94	0.92	+1.69	+1.77	-0.08	3		8	8	8	9	
5187.45	1.20	+1.81	+1.73	+0.08	1		6		5	5	
Pr II	3994.83	0.05	+0.72	+0.81	-0.09		hfs	9		12	12
Nd II 60	4021.34	0.31	+0.97	+1.02	-0.05	1		7	8	9	13
	4023.00	0.20	+1.06	+1.11	-0.05	3		11	10	13	<18>
	4059.96	0.20	+0.79	+0.80	-0.01	3		6		7	7
	4069.28	0.06	+0.72	+0.83	-0.11	2		7		10	13
	4446.39	0.20	+0.80	+0.96	-0.16	1		7	6	11	10
	4462.99	0.55	+1.34	+1.41	-0.07	1		11	10	13	<13>
	4811.34	0.06	+0.45	+0.57	-0.12	5		5	4	7	<10>
	5092.80	0.37	+0.71	+0.77	-0.06	1		5	4	6	6
	5179.78	0.74	+0.88	+0.84	+0.04	2		4	4	3	<8>
	5293.17	0.81	+1.31	+1.39	-0.08	1		8		9	9
5319.82	0.54	+1.08	+1.16	-0.08	5		7	7	9	9	
Sm II 62	4318.94	0.27	+0.68	+0.60	+0.08	3		7		7	11
	4420.53	0.33	+0.47	+0.65	-0.18	1		4		7	9
	4467.34	0.65	+1.16	+1.11	+0.05	3	hfs	11		10	10
	4519.63	0.54	+0.54	+0.61	-0.07	5	hfs	4	4	4	<5>
	4537.95	0.48	+0.51	+0.63	-0.12	1		4	3	5	6
	4566.21	0.33	+0.52	+0.69	-0.17	5	hfs	5	3	9	<8>
	4577.69	0.24	+0.16	+0.20	-0.04	1		3		3	4
	4719.84	0.04	+0.22	+0.27	-0.05	1	hfs	5	3	7	7

For the ionized REE lines, the derived abundances are found to be insensitive to the choice of the models: they are larger by 0.01 dex to 0.02 dex for the Holweger and Müller's model than for the Kurucz's model.

2.3. Spectrum synthesis

All the analyzed lines were treated fully relative to the Sun to minimize the uncertainties in atomic data and the errors in the

computational procedure. Based on the approximation of LTE line formation, we initially synthesized all the solar spectral features which contain the REE lines listed in Table 1. The standard solar composition compiled by Grevesse (1984) was used in this computation.

The method of spectrum synthesis used here is an iterative one which is similar to the Leckrone's (1981) *bootstrap* technique. This technique is employed to "circumvent the problem of large systematic errors in published transition probabilities." We assume

Table 1 (continued)

Elant	λ (Å)	α (eV)	log $gf\epsilon$			Wght	hfs	Computed & Measured EW			
			Procyon	Sun	[ϵ]			Procyon		Sun	
Eu II 63	3724.94	0.00	+0.45	+0.47	-0.02	2	hfs	26		30	21
	3907.10	0.20	+0.56	+0.51	+0.05	1	hfs	22		22	27
	4129.70	0.00	+0.71	+0.73	-0.02	5	hfs	48	38	54	58
	6437.64	1.31	+0.77	+0.79	-0.02	3	hfs	8	8	6	<6>
	6645.11	1.37	+0.76	+0.75	+0.01	2	hfs	6		6	5
Gd II 64	3549.36	0.23	+1.31	+1.42	-0.11	1		15		19	25
	3712.70	0.38	+1.10	+1.12	-0.02	1		10		11	10
	3894.70	0.00	+0.63	+0.59	+0.04	1		8		8	8
	3916.51	0.59	+1.17	+1.18	-0.01	1		8		9	11
	4085.56	0.72	+1.21	+1.18	+0.03	3		8		7	6
Tb II 65	3658.86	0.13	+0.18	+0.19	-0.01		hfs	3		3	<3>
Dy II 66	3407.79	0.00	+1.09	+1.30	-0.21	1		23	37	29	<60>
	3506.81	0.10	+0.94	+1.10	-0.16	1		15	22	21	<46>
	3672.31	0.58	+0.61	+0.73	-0.12	1		4		6	7
	3694.81	0.10	+0.79	+0.81	-0.02	5		15	18	15	17
	4073.15	0.53	+0.67	+0.65	+0.02	4		6	8	6	7
Er II 68	3385.08	0.05	+0.62	+0.88*	-0.26	1		12		19	
	3896.25	0.05	+0.64	+0.75	-0.11	1		17		20	<24>
Tm II 69	3462.20	0.00	+0.23	+0.25	-0.02	2		10		12	16
	3700.26	0.02	-0.32	-0.62	+0.30	1		4		2	4
	3701.36	0.00	-0.40	-0.44	+0.04	3		4		4	3
	3795.76	0.02	-0.05	+0.16	-0.21	1		7		12	<10>
Yb II 70	3694.19	0.00	+0.75	+0.79	-0.04			72		52	(58)
Lu II 71	3397.07	1.45	+0.53	+0.54	-0.01			10		10	(16)

that a set of lines listed by Kurucz and Peytremann (1975) is completely responsible for an observed feature. Solar spectral profiles which were synthesized using these gf values are usually unable to reproduce the observed structures. Then it was assumed, as in Leckrone (1981), that this is due to errors in the Kurucz and Peytremann's (1975) transition probabilities and that their gf values should be modified to match the observations. The modifications of gf values for individual lines were made empirically for the Sun after a number of trials. For some neutral lines rather large modifications of $\log gf$ values up to 1.5 dex were needed, but the corrections for most of the lines were less than that.

Applying these modified solar gf values, we synthesized the spectrum of Procyon. The abundance of REE in question was taken as an unknown free parameter while those of other elements were fixed to the values of Procyon determined in the previous study (Kato and Sadakane, 1982). However, slight modifications less than 0.15 dex (this is within error limits of our analysis) were needed for some absorption lines to achieve the best match with observations in some cases.

The method of spectrum synthesis is superior to the usual method of measuring equivalent width in order to overcome the effects of line blending and broadening due to hfs. However, this statement is not always valid. As illustrated by Grevesse (1969) in a case of misidentification of the solar Bi line, closer attention has to be paid when we use spectrum data obtained with rather large instrumental profiles. In such a case, even the method of synthesis can not reproduce the original form of the spectrum.

3. Results

Columns 4 and 5 of Table 1 give the $\log gf\epsilon$ values for the individual line in Procyon and in the Sun, respectively. These are measured on the usual scale where $\log \epsilon(\text{H}) = 12.0$. The final relative abundances are shown in the column 6 of Table 1 in terms of [ϵ] which is defined by:

$$[\epsilon] = \log (\epsilon/\epsilon(\text{H}))_{\text{Procyon}} - \log (\epsilon/\epsilon(\text{H}))_{\odot}.$$

Columns 9 and 11 of Table 1 give the equivalent widths computed for both stars applying $\log gf\epsilon$ values listed in the columns 4 and 5. Columns 10 and 12 display the measured equivalent widths. We can see fairly good agreements between the computed equivalent widths and the observed ones. This implies that the $\log gf\epsilon$ values obtained here satisfy the observed strengths of the lines. Figure 1 shows the comparison of solar $\log gf\epsilon$ values with those of Grevesse and Blanquet (1969) and Steffen (1985), and similarly Fig. 2 shows the case of Procyon. Our solar values are somewhat greater than those of Grevesse and Blanquet (1969) but they are slightly smaller than those of Steffen (1985). There seems to be a small systematic discrepancy in $\log gf\epsilon$ values of Procyon between ours and Steffen's (1985).

We describe below some details of the analysis which are specific to individual elements.

La: Four La II lines seem to be widened by hyperfine splitting. However, we can not take it into consideration exactly because we have no hfs data of these lines. The La abundance was

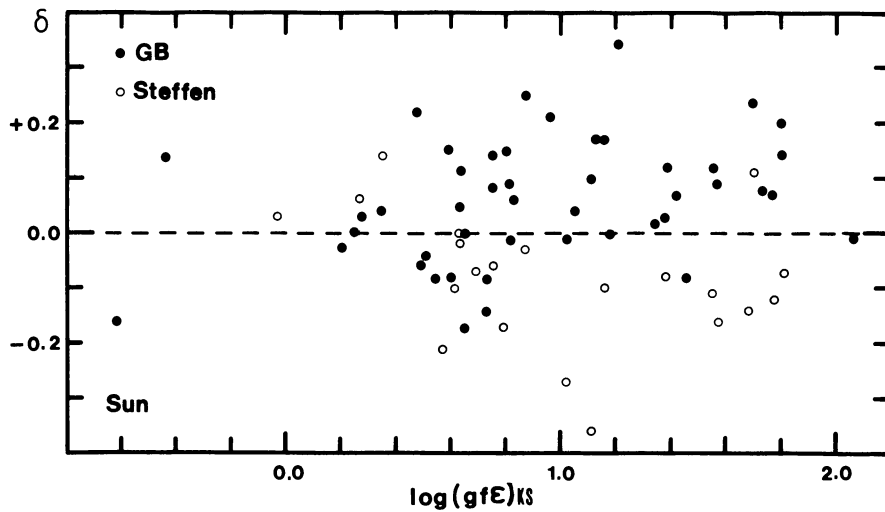


Fig. 1. A comparison of the solar $\log gf\epsilon$ values of this study with those of two previous analyses (Grevesse and Blanquet, 1969; Steffen, 1985). The abscissa is $\log gf\epsilon$ values of this study; the ordinate is $\delta = (\log gf\epsilon)_{\text{this study}} - (\log gf\epsilon)_{\text{others}}$

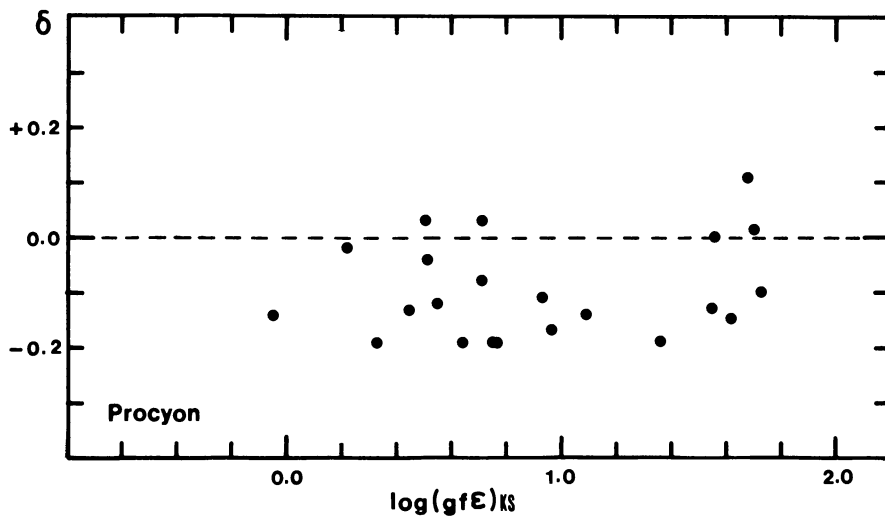


Fig. 2. A comparison of the Procyon's $\log gf\epsilon$ values of this study with those of Steffen (1985). $\delta = (\log gf\epsilon)_{\text{this study}} - (\log gf\epsilon)_{\text{Steffen}}$

schematically deduced assuming that each La II line has three to nine hyperfine components. The intensity ratios among them were determined from the condition that the computed solar feature matches the observed profile.

Pr: The only detectable Pr II line is at 3994.83 Å; it was studied in detail by Biéumont et al. (1979) for the Sun. Six split lines between 3994.69 Å and 3994.88 Å are overlapped on the wing of a strong Ti I line at 3994.68 Å. In addition, there is a weak Ni I line at 3994.80 Å. In Fig. 3, the contribution of the Pr II is demonstrated for Procyon.

Sm: The hyperfine splitting was taken into account for the lines at 4467.34 Å and 4519.63 Å (Ekeland and Hauge, 1975), while the effect for the other lines was schematically treated in the same manner as for La.

Eu: Hauge (1972) has studied the solar isotope ratio of Eu from the analysis of the lines widened by the hfs. We could confirm his result (a logarithmic isotope ratio $\log(\epsilon(\text{Eu}^{153})/\epsilon(\text{Eu}^{151}))$ of -0.25) for the line 4129.70 Å and then the same procedure was applied to Procyon. We find the logarithmic isotope ratio to be in the range from -0.50 to -0.10 . This may lead to the conclusion that the isotopic composition of Eu in Procyon is similar to the solar value.

Gd, Dy, Tm: Results for these three elements are rather uncertain because most of the lines are in the wavelength region

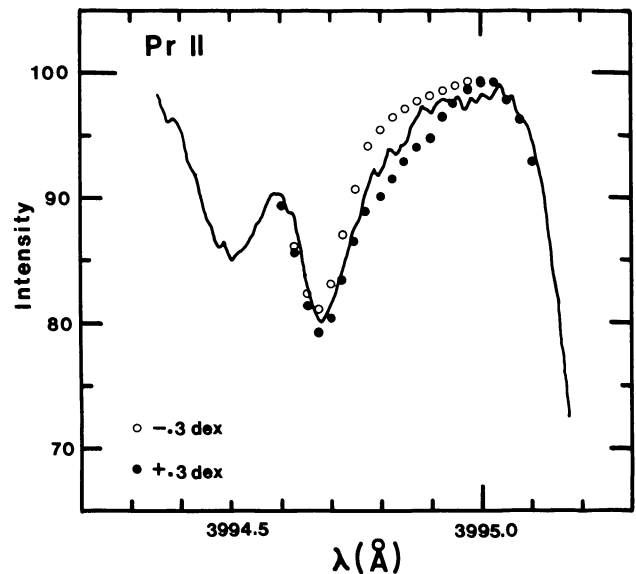


Fig. 3. Spectrum of Procyon around the Pr II 3994.83 Å line (full line). Synthesized profiles for the two cases (over- and under-abundant by 0.3 dex with respect to the adopted $\log gf\epsilon$ value) are also shown for comparison

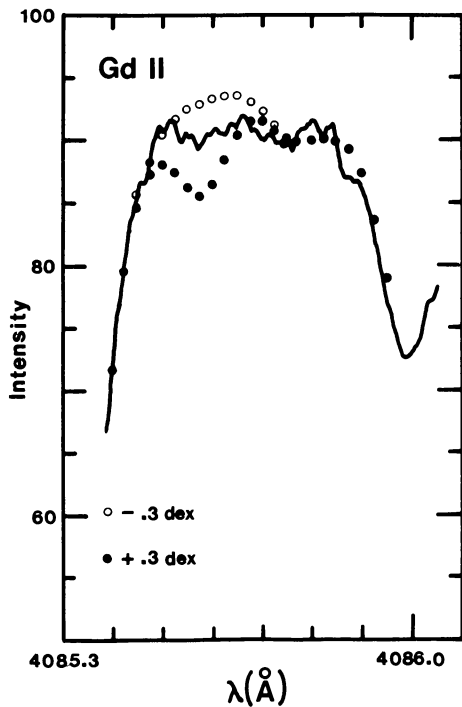


Fig. 4. Spectrum of Procyon around the Gd II 4085.56 Å line (full line). Synthesized profiles are also shown for comparison

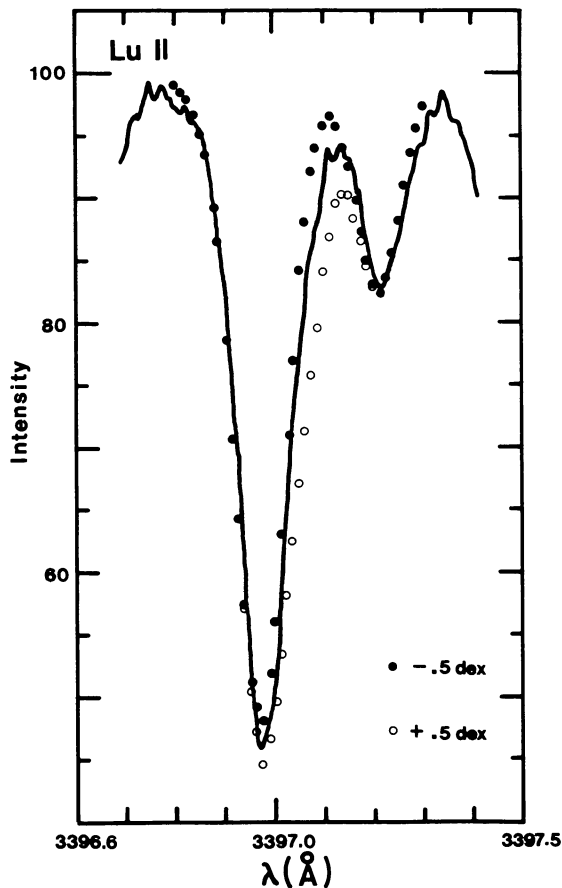


Fig. 5. Spectrum of Procyon around the Lu II 3397.07 Å line (full line). Synthesized profiles are also shown for comparison

Table 2. Composition [ϵ] of rare-earth elements in Procyon. N is the number of lines used, and $\Delta\epsilon$ is the distribution of $\log gf\epsilon$ values in Table 1. The last three columns are assigned to the results determined by other investigators (Steffen, 1985; Kato and Sadakane, 1982; Griffin, 1971)

Elant	N	[ϵ]	$\Delta\epsilon$	Steffen	KS(82)	Griffin
57 La	10	-0.05	0.15	0.22	-0.01	-0.3
58 Ce	12	-0.03	0.17	-0.08	-0.09	-0.2
59 Pr	1	-0.09	--			
60 Nd	11	-0.08	0.20	-0.14	-0.25	-0.3
62 Sm	8	-0.06	0.26	-0.10	-0.31	-0.4
63 Eu	5	-0.01	0.07	0.03	-0.14	-0.3
64 Gd	5	-0.00	0.15			
65 Tb	1	-0.01	--			
66 Dy	5	-0.04	0.23		-0.40	
68 Er	2	-0.19	0.15			
69 Tm	4	+0.02	0.51			
70 Yb	1	-0.04	--			
71 Lu	1	-0.01	--			

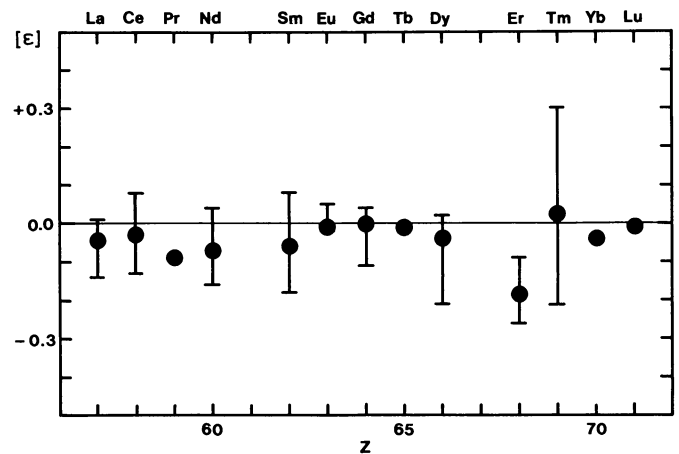


Fig. 6. REE abundances in Procyon relative to the Sun

below 4000 Å where many lines are crowded. Figure 4 shows the contribution of the Gd II line at 4085.56 Å in the wing of H δ .

Tb: The information on the line at 3658.86 Å is obtained from Biémont et al. (1981). The solar $\log gf\epsilon$ value (+0.19) in Table 1 is somewhat too small when compared with them. We have no definite idea to explain this discrepancy. One possible explanation is the difference of the adopted partition function. We used Irwin's (1981) polynomial representation in this analysis.

Er: The solar Er abundance is investigated by Biémont and Youssef (1984). The solar $\log gf\epsilon$ value of 3385.08 Å line in Table 1 is adopted from their result.

Yb, Lu: Only one line can be detected for these elements. Lu is certainly present in Procyon. Figure 5 shows the appearance of the Lu II line at 3397.07 Å.

4. Discussion

The final result is presented in Table 2 and in Fig. 6. We can see good agreement of the REE abundances in Procyon with those in

the Sun. The uncertainties indicated represent the span of the individual relative abundances [ε] in Table 1.

The main result of the present analysis is that the rare-earth elements of Procyon show the solar abundance pattern. The mean relative abundance derived from our analysis is -0.04 dex and the standard deviation is 0.05 dex.

As noted in Sect. 2, there is a slight systematic difference between the $\log gf\varepsilon$ values obtained in this study and those of Steffen (1985). But it is only a virtual one. The effective temperature (6750 K) adopted by Steffen is higher by 100 K than ours. If we take this higher effective temperature into account, a somewhat larger (about $+0.05$ dex) $\log gf\varepsilon$ value can be obtained. In addition he corrected "measured" equivalent widths to obtain "true" ones. He found that a correction of about 10% is necessary for weak lines. In this analysis this effect was entirely ignored and it was assumed that the line profiles on the *Procyon Atlas* show the real observed contour. If we take the correction into account, a larger $\log gf\varepsilon$ values (about $+0.05$ dex) will be obtained. When the Steffen's procedure is adopted, the relative abundances shown in Table 2 and in Fig. 6 have to be raised by 0.1 dex. Therefore a systematic difference in Fig. 2 will disappear through these corrections.

On the other hand our results disagree with the values obtained by Leushin and Sokolov (1982). They derived overabundances of the REE in Procyon assuming a rather lower effective temperature of 6385 K. The discrepancy can hardly be explained by the difference in the temperature.

The splitting of lines due to hyperfine structure is also important especially for a moderately strong line such as 3988.52 Å line of La II (equivalent width W_λ is 45 mÅ) and 4129.70 Å line of Eu II (W_λ is about 50 mÅ). As shown by Booth and Blackwell (1983) and Whaling et al. (1985), an erroneous $\log gf\varepsilon$ value can be obtained, if the effect of hfs is ignored. As another example, we show the case of Eu II line at 4129.70 Å which has 12 hyperfine components. We obtain $\log gf\varepsilon$ values of 1.38 and 0.91 for the Sun and Procyon respectively, when we assume the line consists of only one component. These are considerably larger than the values (0.73 and 0.71) listed in Table 1 and the relative abundance of Procyon reduces by 0.45 dex (about 1/3!). A strong line is formed in the cooler upper atmosphere, while splitted weak components originate from rather warm deeper layers. Therefore a simple convolution of gf values of each component fails to reproduce the observed line strength.

Abundance studies of REE provide information on nucleosynthesis during the last stages of stellar evolution. More observational studies for other stars of various ages based on

high enough quality data are necessary to discuss the interesting history of the formation of rare-earth elements in the galactic disk.

Acknowledgements. We would like to thank Dr. G. Roland, Institut d'Astrophysique de l'Université de Liège, for providing us with the unpublished intensity tracings of the solar spectrum. We are indebted to Dr. N. Grevesse for valuable comments on the original manuscript as a referee. This research was partly supported by the Scientific Research Fund of the Ministry of Education, Science, and Culture under grant No. 59914013.

References

- Biémont, E., Grevesse, N., Hauge, Ø.: 1979, *Solar Phys.* **61**, 17
 Biémont, E., Roland, G., Delbouille, L.: 1981, *Solar Phys.* **71**, 223
 Biémont, E., Youssef, N.Y.: 1984, *Astron. Astrophys.* **140**, 177
 Booth, A.J., Blackwell, D.E.: 1983, *Monthly Notices Roy. Astron. Soc.* **204**, 777
 Delbouille, L., Roland, G., Neven, L.: 1973, Photometric Atlas of the Solar Spectrum from $\lambda 3000$ to $\lambda 10000$, Institut d'Astrophysique de l'Université de Liège
 Edmonds, F.N.: 1964, *Astrophys. J.* **140**, 902
 Ekeland, A., Hauge, Ø.: 1975, *Solar Phys.* **42**, 17
 Gray, D.F.: 1977, *Astrophys. J.* **218**, 530
 Grevesse, N.: 1969, *Solar Phys.* **6**, 381
 Grevesse, N.: 1984, *Physica Scripta* **T8**, 49
 Grevesse, N., Blanquet, G.: 1969, *Solar Phys.* **8**, 5
 Griffin, R.: 1971, *Monthly Notices Roy. Astron. Soc.* **155**, 139
 Griffin, R. and R.: 1979, A Photometric Atlas of the Spectrum of Procyon, R. and R. Griffin, Cambridge, England
 Hauge, Ø.: 1972, *Solar Phys.* **27**, 286
 Holweger, H., Müller, E.A.: 1974, *Solar Phys.* **39**, 19
 Irwin, A.W.: 1981, *Astrophys. J. Suppl.* **45**, 621
 Kato, K., Sadakane, K.: 1982, *Astron. Astrophys.* **113**, 135
 Kurucz, R.L.: 1979, *Astrophys. J. Suppl.* **40**, 1
 Kurucz, R.L., Peytremann, E.: 1975, *Smithsonian Ap. Obs. Spec. Rept.*, No. 362
 Leckrone, D.S.: 1981, *Astrophys. J.* **250**, 687
 Leushin, V.V., Sokolov, V.V.: 1982, *Bulletin of the Crimean Astrophys. Obs.* **62**, 34
 Moore, C.E., Minnaert, M.G.J., Houtgast, J.: 1966, *Natl. Bur. Stand. Monogr.*, No. 61
 Steffen, M.: 1985, *Astron. Astrophys. Suppl.* **59**, 403
 Whaling, W., Hannaford, P., Lowe, R.M., Biémont, E., Grevesse, N.: 1985, *Astron. Astrophys.* **153**, 109